Designation: F 996 – 98 (Reapproved 2003)

Standard Test Method for Separating an Ionizing Radiation-Induced MOSFET Threshold Voltage Shift Into Components Due to Oxide Trapped Holes and Interface States Using the Subthreshold Current–Voltage Characteristics[1]

This standard is issued under the fixed designation F 996; the number immediately following the designation indicates the year of original adoption or, in the case of revision, the year of last revision. A number in parentheses indicates the year of last reapproval. A superscript epsilon (ε) indicates an editorial change since the last revision or reapproval.

1. Scope

1.1 This test method covers the use of the subthreshold charge separation technique for analysis of ionizing radiation degradation of a gate dielectric in a metal-oxide-semiconducter-field-effect transistor (MOSFET) and an isolation dielectic in a parasitic MOSFET.[2, 3, 4] The subthreshold technique is used to separate the ionizing radiation-induced inversion voltage shift, ΔV_{INV} into voltage shifts due to oxide trapped charge,ΔV_{ot} and interface traps,ΔV_{it}. This technique uses the pre- and post-irradiation drain to source current versus gate voltage characteristics in the MOSFET subthreshold region.

1.2 Procedures are given for measuring the MOSFET subthreshold current-voltage characteristics and for the calculation of results.

1.3 The application of this test method requires the MOSFET to have a substrate (body) contact.

1.4 Both pre- and post-irradiation MOSFET subthreshold source or drain curves must follow an exponential dependence on gate voltage for a minimum of two decades of current.

1.5 The values given in SI units are to be regarded as standard. No other units of measurement are included in this test method.

1.6 *This standard does not purport to address all of the safety concerns, if any, associated with its use. It is the responsibility of the user of this standard to establish appropriate safety and health practices and determine the applicability of regulatory limitations prior to use.*

2. Terminology

2.1 *Definitions of Terms Specific to This Standard:*

2.1.1 *anneal conditions*—the bias and temperature of the MOSFET in the time period between irradiation and measurement.

2.1.2 *doping concentration, N*—*N*- or *P*-type doping, is the concentration of the MOSFET channel region adjacent to the oxide/silicon interface.

2.1.3 *inversion current, I_{INV}*—the MOSFET channel current at a gate-source voltage equal to the inversion voltage.

2.1.4 *inversion voltage, V_{INV}*—the gate-source voltage corresponding to a surface potential of $2\phi_B$.

2.1.5 *irradiation biases*—the biases on the gate, drain, source, and substrate of the MOSFET during irradiation.

2.1.6 *midgap current, I_{MG}*—the MOSFET channel current at a gate-source voltage equal to the midgap voltage.

2.1.7 *midgap voltage, V_{MG}*—the gate-source voltage corresponding to a surface potential of ϕ_B.

2.1.8 *oxide thickness, t_{ox}*—the thickness of the oxide of the MOSFET under test.

2.1.9 *potential, ϕ_B*—the potential difference between the Fermi level and the intrinsic Fermi level.

2.1.10 *subthreshold swing*—the change in the gate-source voltage per change in the log source or drain current of the MOSFET channel current below the inversion current. The value of the subthreshold swing is expressed in V/decade (of current).

2.1.11 *surface potential, ϕ_s*—the potential at the MOSFET semiconductor surface measured with respect to the intrinsic Fermi level.

3. Summary of Test Method

3.1 The subthreshold charge separation technique is based on standard MOSFET subthreshold current-voltage characteristics. The subthreshold drain or source current at a fixed drain to source voltage, V_{DS}, is measured as a function of gate voltage from the leakage current (or limiting resolution of the

[1] This test method is under the jurisdiction of ASTM Committee F01 on Electronics and is the direct responsibility of Subcommittee F01.11 on Quality and Hardness Assurance.

Current edition approved May 10, 1998. Published September 1998. Originally published as F 996 – 91. Last previous edition F 996 – 92.

[2] For formulation of subthreshold charge separation technique see McWhorter, P. J. and P. S. Winokur, "Simple Technique for Separating the Effects of Interface Traps and Trapped Oxide Charge in MOS Transistors," *Applied Physics Letters*, Vol 48, 1986, pp. 133–135.

[3] DNA-TR-89-157, Subthreshold Technique for Fixed and Interface Trapped Charge Separation in Irradiated MOSFETs, available from National Technical Information Service, 5285 Port Royal Rd., Springfield, VA 22161.

[4] Saks, N. S., and Anacona, M. G., "Generation of Interface States by Ionizing Radiation at 80K Measured by Charge Pumping and Subthreshold Slope Techniques," *IEEE Transactions on Nuclear Science*, Vol NS–34, No. 6, 1987, pp. 1348–1354.

measurement apparatus) through inversion. The drain current and gate voltage are related by $I_D \alpha\ 10^{V_G}$. When plotted as log I_D versus V_G, the linear *I-V* characteristic can be extrapolated to a calculated midgap current, I_{MG}. By comparing the pre- and post-irradiation characteristics, the midgap voltage shift, ΔV_{MG} can be determined. The value of ΔV_{MG} is equal to ΔV_{ot}, which is the voltage shift due to oxide trapped charge. The difference between the inversion voltage shift, ΔV_{INV}, and ΔV_{MG} is equal to ΔV_{it}, which is the voltage shift due to interface traps. This procedure is shown in Fig. 1 for a *p*-channel MOSFET.

4. Significance and Use

4.1 The electrical properties of gate and field oxides are altered by ionizing radiation. The time dependent and dose rate effects of the ionizing radiation can be determined by comparing pre- and post-irradiation voltage shifts, ΔV_{ot} and ΔV_{it}. This test method provides a means for evaluation of the ionizing radiation response of MOSFETs and isolation parasitic MOSFETs.

4.2 The measured voltage shifts, ΔV_{ot} and ΔV_{it}, can provide a measure of the effectiveness of processing variations on the ionizing radiation response.

4.3 This technique can be used to monitor the total-dose response of a process technology.

5. Interferences

5.1 *Temperature Effects*—The subthreshold drain current varies as the exponential of $q\phi_B/kT$, and other terms which vary as a function of temperature. Therefore, the temperature of the measurement should be controlled to within ±2°C, since the technique requires a comparison of pre- and post-irradiation data. At cryogenic temperatures, this test method may give misleading results. [4]

5.2 *Floating Body (Kink) Effects*—Floating body effects occur in MOSFETs without body (substrate) ties. This test method should not be applied to a MOSFET without a substrate or substrate/source contact.

5.3 *Short Channel Effects*—To minimize drain voltage dependence on the subthreshold curve, a small drain measurement voltage is recommended but not necessary.

5.4 *Leakage Current*—Because the MOSFET midgap current is below the capabilities of practical current-voltage measurement instrumentation, extrapolation of the subthreshold swing is required for the determination of a MOSFET midgap voltage. Extrapolation of ideal linear MOSFET subthreshold current-voltage characteristics is unambiguous, because of the constant subthreshold swing. An example of near ideal subthreshold characteristics is given in Fig. 2, where the subthreshold swing is relatively constant between 10^{-11} and 10^{-6} A. Nonideal subthreshold characteristics, that are aberrations from the theoretical linear subthreshold swing, can complicate the subthreshold swing extrapolation to the midgap voltage. For subthreshold characteristics that have multiple subthreshold swings, the value of the midgap voltage would be dependent on the values of the subthreshold current from which the extrapolation is made. Nonideal subthreshold characteristics are caused by MOSFET leakage currents that can be either independent of, or a function of, gate-source voltage.

5.4.1 *Junction Leakage Current*—This leakage current is from the drain to the substrate and is independent of gate-source voltage. Junction leakage current masks the actual MOSFET channel subthreshold current below the leakage current level. Junction leakage current is easily distinguished from the channel subthreshold current as is shown in Fig. 2 by the flat section of the drain current, I_D, below 10^{-11} A. This figure also shows the advantage of using the source current, I_S, for extrapolation. The source current is not affected by junction leakage so that a measure of the MOSFET channel current is obtained to the instrumentation noise level. However, if there is not a separate source and substrate contact (for example, power MOSFETs), the drain current must be used. Only the part of the subthreshold curve above the junction leakage or instrumentation noise level should be used for extrapolation. A minimum of two decades of source or drain current above the leakage or noise is required for application of this test method.

5.4.2 *Gate Leakage*—Gate leakage can be any combination of leakage from the gate to source, drain, or substrate. Typically this leakage will be a function of the gate-source voltage. If gate leakage is greater than 1.0 μA for any gate-source voltage, the test method should not be applied. Gate leakages less than 1.0 μA can still cause nonideal

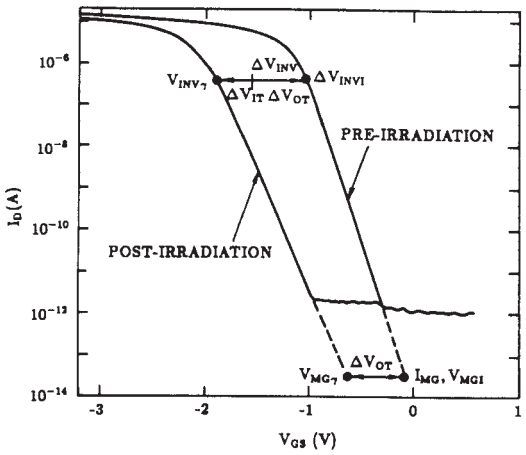

FIG. 1 Determination of Radiation Induced Voltage Shift for *p*-Channel MOSFET

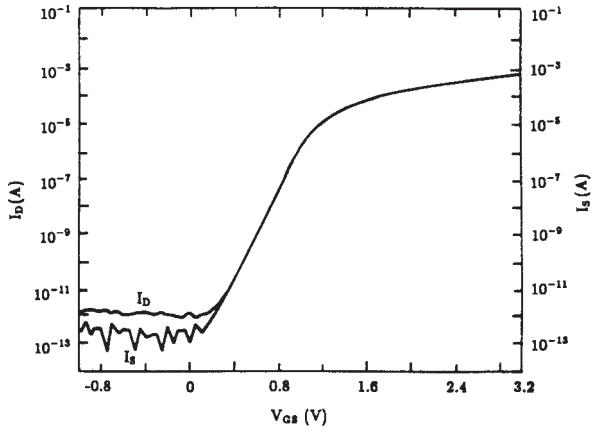

FIG. 2 Near Ideal Subthreshold Characteristics from an *n*-Channel Transistor

subthreshold characteristics. The minimum value of the subthreshold source or drain current used for extrapolation to the midgap voltage must be above any changes in the subthreshold swing that can be attributed to gate leakage. Plotting the log of the gate leakage along with log source and drain current on the same graph, will aid in the determination of gate leakage effects on the drain and source subthreshold swing.

5.4.3 *Edge Leakage Current*—Most microcircuit MOSFETs use an open geometry layout so that ionizing radiation induced drain to source leakage can occur in *n*-channel devices outside of the intentional MOSFET channel. The effect of this edge leakage on the subthreshold swing is dependent on the aspect ratios and threshold voltages of the intentional and parasitic MOSFETs. The aspect ratio of the parasitic MOSFET would usually be much smaller than a standard width MOSFET layout. Thus, when the MOSFET channel is in strong inversion, the channel current will typically dominate. However, as the channel current is reduced, edge leakage can go from a minimal fraction to dominating the measured drain or source current if the parasitic MOSFET inversion voltage is less than the intentional MOSFET. This effect can be observed in the measured subthreshold characteristics as a deviation from the ideal linear subthreshold curve that is a function of the gate-source voltage. Examples of parasitic MOSFET induced deviations from the ideal linear subthreshold swing are given in Fig. 3 and Fig. 4. In Fig. 3, the subthreshold swing changes from the initial swing near inversion to a much larger mV/decade swing. In Fig. 4, a more pronounced deviation is shown. The section of the subthreshold curve that should be used for extrapolation to the midgap voltage is shown in both figures. The upper section of the subthreshold curve above the lower current level deviations was used. Any lower current change in the subthreshold swing from the initial subthreshold swing below strong inversion should be considered a parasitic MOSFET induced deviation. Only the part of the subthreshold curve above this deviation should be used for extrapolation as is shown in Fig. 3 and Fig. 4. Some *n*-channel MOSFETs may have post-irradiation edge leakage sufficiently large to prevent any observation of a subthreshold swing. The subthreshold charge separation technique cannot be applied to these samples. A minimum of two decades of source or drain current

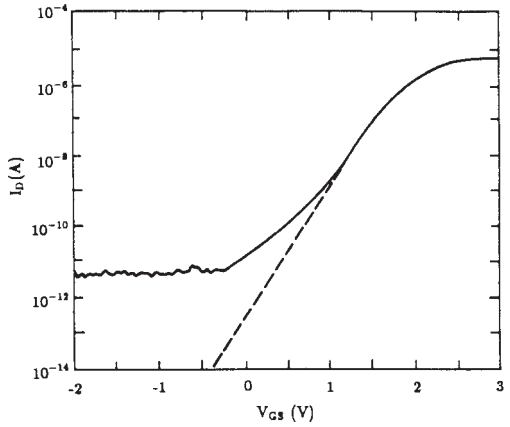

FIG. 3 Example of a Parasitic MOSFET Induced Deviation From the Ideal Linear Subthreshold Swing

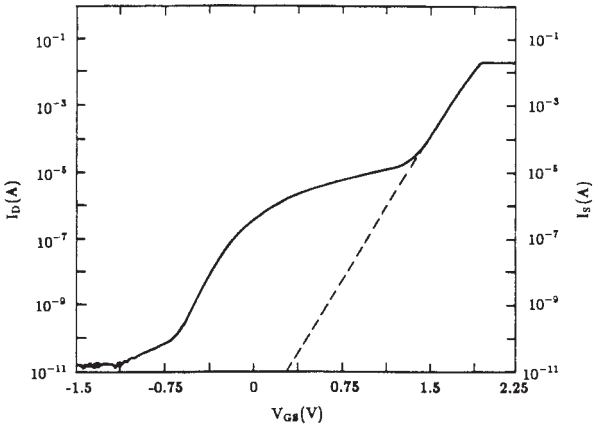

FIG. 4 Example of a Parasitic MOSFET Induced Deviation from the Ideal Linear Subthreshold Swing

above any subthreshold swing deviation is required for application of this test method. Open and closed (annular) geometry layouts can be used to separate edge leakage current from the MOSFET channel current.

5.4.4 *Backchannel and Sidewall Leakage in a SOI MOSFET*—Backchannel leakage arises from a parasitic MOSFET located at the interface between the epitaxial silicon and the insulator. Sidewall leakages arise from the parasitic MOSFET formed at the edges of the intentional MOSFET. These parasitics distort the subthreshold curve in the same manner as described in 5.4.3.

6. Apparatus

6.1 To measure the subthreshold current-voltage characteristics of a MOSFET, the instrumentation required consists of, as a minimum, two voltage sources and four ammeters.

6.2 The power supplies are used to apply voltage to the gate and drain of the MOSFET. The ammeters are used to measure the gate, drain, source, and substrate currents.

6.3 For MOSFETs that have a common source/substrate contact, only three ammeters are required.

6.4 For a typical digital microcircuit MOSFET the voltage sources and ammeters should meet the specification given in Table 1.

6.5 For a power, parasitic field oxide, or high voltage linear MOSFET, the maximum voltage requirement for the gate-source power supply can be substantially larger. Field oxide field effect transistor (FET)s may have pre-irradiation threshold voltages of several hundred volts. The gate-source power supply is required to be such that the MOSFET drain-to-source subthreshold current can be measured from leakage into strong inversion. The resolution of a gate-source power supply must be at least 0.5 % of the maximum gate-source voltage, for the MOSFET subthreshold current-voltage measurement.

6.6 The test fixture, containing the MOSFET under test (DUT), and the cabling connecting the test instrumentation,

TABLE 1 Minimal Instrumentation Specifications

Drain-source power supply	±10 V, 0.01 V resolution
Gate-source power supply	±10 V, 0.005 V resolution
Ammeters	±10 mA, 10 pA resolution

must be designed for low current measurements specified in Table 1. Probe stations can be used for MOSFETs in wafer form as long as a current resolution of 100 pA can be maintained.

6.7 The test fixture may be the same or different from the fixture(s) used during irradiation and anneal (irradiation and anneal fixture(s)). Any handling of the DUT must be performed so as to minimize static discharge or other voltage transients that may damage (alter current-voltage characteristics) the DUT.

6.8 For control of measurement and data recording, the subthreshold current-voltage characteristics can be measured with a programmable tester having the proper current and voltage capabilities, or with computer control of independent power supplies and ammeters. To minimize apparatus setup, programmable testers are usually selected.

7. Test Specimens and Sampling

7.1 *Test Specimens*— This test method can be applied to MOSFETs in wafer form using a probe station or in package form.

7.2 *Sampling*—This test method determines the properties of a single MOSFET. If sampling procedures are used to select MOSFETs for test, they must be agreed upon in advance by the parties to the test.

8. Calibration

8.1 Determine the current noise levels of the apparatus for measuring the MOSFET current-voltage characteristics. Perform a gate-source voltage sweep without a DUT in the test fixture. If a probe station is being used, move the probes into the proximity of each other which would be representative of probing of the actual MOSFET. Record the gate, drain, source, and substrate current noise levels.

9. Test Conditions

9.1 This test method only describes the application of the subthreshold charge separation technique. The total-dose irradiation test procedure, which, for example, includes the type of irradiation exposure, the total-dose measurement interval(s), the irradiation bias condition, the anneal bias condition, and the time between irradiation and test, must be agreed upon in advance by the parties to the test.

9.2 *MOSFET Type—p*-channel or *n*-channel.

9.3 Before this test method can be implemented, the gate-source and drain-source voltages that are appropriate for the MOSFET type to be measured must be selected. These vary from one MOSFET type to another.

9.3.1 The magnitude of the drain-source voltage used to measure the subthreshold is recommended to be between 100 and 150 mV or the microcircuit V_{cc}. The drain-source voltage is positive for an *n*-channel and negative for a *p*-channel. Since the drain-source voltage, V_{DS}, can influence the subthreshold current-voltage characteristics because of short channel effects, V_{DS} must be agreed upon in advance by the parties to the test.

9.3.2 The gate-source voltage sweep range is adjusted to measure the MOSFET subthreshold from leakage to a channel current that is at least ten times the inversion current, I_{INV}. The gate-source voltage step size is adjusted so that a minimum of two or three drain and source currents are measured per decade of subthreshold current.

9.3.3 The source and substrate are grounded.

9.4 Measure the DUT subthreshold current-voltage characteristics.

9.5 Determine the suitability of the application of this test method to the DUT. Base the decision on the existence and magnitude of the leakage currents discussed in 5.4.

9.5.1 Plot the log of all DUT currents versus the gate-source voltage on the same graph for comparison. The purpose of plotting all currents is to analyze the DUT for junction and gate leakage paths, and parasitics that can cause distortions of the subthreshold drain or source curves, or both (see 5.4).

9.5.2 If the DUT is found unacceptable for this test method, choose a new sample and return to 9.3.

9.6 Decide on whether the source or drain current will be used for application of this test method. Use the source current, unless the source and substrate contacts are common or if the subthreshold drain current has less junction and gate leakage current than the source current. For these two cases, use the drain current.

10. Procedure

10.1 *Pre-Irradiation Characterization*:

10.1.1 Select the circuit configuration for subthreshold measurement (see 9.2).

10.1.2 Program the gate-source voltage range and the drain-source voltage (if applicable) to measure the DUT subthreshold current-voltage characteristics (see 9.3).

10.1.3 Insert the DUT into the test fixture.

10.1.4 Measure the DUT subthreshold current-voltage characteristics. Record the gate, drain, source, and substrate currents (providing all contacts are available) versus the gate-source voltage.

10.1.5 If necessary, remove the DUT from test fixture and insert the DUT into the irradiation fixture (see 6.7).

10.1.6 Apply irradiation bias as soon as possible and perform DUT irradiation.

10.2 *Post-Irradiation Characterization*:

10.2.1 If necessary, remove the DUT from the irradiation fixture and insert the DUT into the test fixture (see 6.7).

10.2.2 Adjust the programmed gate-source voltage range (if applicable) to compensate for the ionizing radiation-induced inversion voltage shift (see 9.3.2).

10.2.3 Measure the DUT subthreshold current-voltage characteristics. Record the gate, drain, source, and substrate currents versus the gate-source voltage.

10.2.4 If irradiation or anneal testing, or both, are to continue, perform the next two steps.

10.2.4.1 If necessary, remove DUT from test fixture and insert in the irradiation fixture or an anneal fixture (see 6.7).

10.2.4.2 Apply irradiation or anneal bias as soon as possible and perform DUT irradiation if applicable.

11. Calculation

11.1 Perform all test method calculations using the DUT source or drain current, I_c, based on the decision in 9.5.

11.2 *Calculate a Value for the Transconductance*—The value of the transconductance is obtained from the pre-irradiation I_c and the gate-source voltage, $V_{G\ S}$, data. The pre-irradiation value of transconductance is used in the analysis of all the post-irradiation and anneal measurements.

11.2.1 The value of the transconductance, G_M, is the maximum slope from the plot of the pre-irradiation I_c versus V_{GS} data. The value of the transconductance can be more easily obtained from the plot of the pre-irradiation $\Delta I_c/\Delta V_{GS}$ versus V_{GS}. The maximum value of$\Delta I_c/\Delta V_{GS}$ corresponds to the maximum slope from the I_c versus V_{GS} plot.

11.2.2 Determine the value of V_{GS} that corresponds to the chosen value of G_M. If the value of G_M is constant for a range of V_{GS}, then use the minimum value of V_{GS}. If:

$$V_{DS} < V_{GS} - V_{INV},$$

the MOSFET is in the linear region of operation, that is normally the case for a V_{DS} of 100 to 150 mV. If:

$$V_{DS} \geq V_{GS} - V_{INV},$$

the MOSFET is in the saturated region of operation.

11.2.3 If the MOSFET is in the linear region of operation, then:

$$K = G_M/V_{DS}.$$

11.2.4 If the MOSFET is in the saturation region of operation, then:

$$K = G_M/(V_{GS} - V_{INV}).$$

11.2.5 An example of a plot of $\Delta\ I_c/\Delta V_{GS}$ versus V_{GS} is given in Fig. 5. The maximum value from this plot is the value of G_M used to solve for K.

11.3 *Calculate Midgap and Inversion Currents*:

11.3.1 Obtain values for N and t_{ox} from the semiconductor facility that processed the DUT. Approximate values can be used for these parameters. A factor of 3 error in N is usually sufficient for a ±5 % error in ΔV_{ot} andΔV_{it}.

11.3.2 The values of midgap and inversion currents, I_{MG} and I_{INV}, are found from the following equations:

$$I_{MG} = K\frac{a}{2\beta^{\,2}}\left(\frac{n_i}{N}\right)^{2}\frac{e^{\,\beta\phi B}}{(\beta\phi_{\,B} - 1)^{\,1/2}} \quad (1)$$

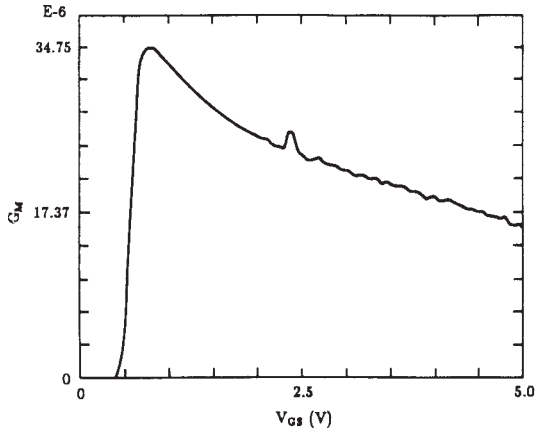

FIG. 5 Plot of G_M Versus Gate Voltage for Drain Voltage of 0.1 V

$$I_{INV} = K\frac{a}{2\beta^{\,2}}\left(\frac{n_i}{N}\right)^{2}\frac{e^{\,2\beta\phi B}}{(2\beta\phi_B - 1)^{\,1/2}} \quad (2)$$

$$a = \frac{\sqrt{2}\epsilon_s t_{ox}}{\epsilon_{\,ox} L_D} \quad (3)$$

$$L_D = \left(\frac{kT\epsilon_s}{Nq^{\,2}}\right)^{1/2} \quad (4)$$

$$\phi_B = \frac{kT}{q}\ln\left(\frac{N}{n_i}\right) \quad (5)$$

$$\beta = \frac{q}{kT} \quad (6)$$

where:

$n_{\,i}$ = intrinsic carrier concentration = $1.01 \times 10^{\,10}$ cm^{-3} $(300\ K) = 3.87 \times 10^{\,16}\ T^{\,3/2} \exp(-0.605\ q/kT)\ cm^{-3}$,

ϵ_s = silicon dielectric constant = $1.05 \times 10^{\,-12}$ F/cm,

ϵ_{ox} = oxide (insulator) dielectric constant = $3.45 \times 10^{\,-13}$ F/cm,

q = elementary charge = $1.60 \times 10^{-19} C$,

k = Boltzmann constant = 1.38×10^{-23} J/K, and

T = temperature in Kelvin.

11.3.3 The values of the midgap and inversion currents calculated from the pre-irradiation MOSFET data are used in the calculation ofΔV_{INV} and ΔV_{MG} for all post-irradiation and anneal measurements.

11.4 Calculate ΔV_{INV}. This calculation is performed for each post-irradiation and anneal measurement.

11.4.1 Find the pre-irradiation value of the inversion voltage, V_{INVI}. The value of V_{INVI}, that corresponds to the calculated value of I_{INV}, is found from the pre-irradiation I_c versus V_{GS} data by using linear interpolation between the two closest measurements on either side of the inversion current, I_{INV}.

11.4.2 Find the post-irradiation value of the inversion voltage, $V_{INV\gamma}$. The value of $V_{INV\gamma}$ is found from the post-irradiation $I_{\,c}$ versus V_{GS} data using linear interpolation as in 11.4.1.

11.4.3 The value of ΔV_{INV} is given by:

$$\Delta V_{INV} = V_{INV\gamma} - V_{INVI}.$$

11.5 Calculate ΔV_{MG}. This calculation is performed for each post-irradiation and anneal measurement.

11.5.1 Find the pre-irradiation value of midgap voltage, V_{MGI}. The value of V_{MGI} is found from the pre-irradiation log $I_{\,c}$ versus V_{GS} data by extrapolation to the calculated midgap current, I_{MG}. Because the value of the midgap current is typically much less than the measurement accuracy of the apparatus, the value of midgap voltage is found by extrapolation of the linear section of the subthreshold log I_C versus $V_{\,GS}$ curve to the value of the midgap current as shown in Fig. 1 through Figs. 3 and Fig 4 (see 5.4). Extrapolate the subthreshold curve to the midgap current, I_{MG}, using a linear least squares fit to the I_c data. The maximum and minimum values of I_c data used for the least squares fit can be defined by the parties to the test or by the user (see 11.1). The minimum and maximum I_c values must be on the linear section of the

subthreshold curve (see 5.4). These values can be determined after the irradiation of the DUT and must be identical for the pre-irradiation and all post-irradiation measurements used in the calculation of results.

11.5.2 Find the post-irradiation value of midgap voltage, $V_{MG\gamma}$. The value of $V_{MG\gamma}$ is found from the pre-irradiation log I_c versus V_{GS} data by extrapolation of the linear least squares fit to the calculated midgap current (see 11.5.1).

11.5.3 The value of ΔV_{MG} is given by:

$$\Delta V_{MG} = V_{MG\gamma} - V_{MGI}.$$

11.6 The values for the radiation induced voltage shift due to oxide trapped charge, ΔV_{ot}, and the voltage shift due to interface traps, ΔV_{it}, are given by:

$$\Delta V_{ot} = \Delta V_{MG}$$

and

$$\Delta V_{it} = \Delta V_{INV} - \Delta V_{MG}.$$

These values are obtained for each post-irradiation and anneal measurement.

12. Report

12.1 Describe the facility used to irradiate the DUT(s) by the following information:

12.1.1 Type of facility (for example, x-ray or ^{60}Co), and

12.1.2 Dose rate in rd(SiO_2)/s.

12.2 For each DUT, report the following:

12.2.1 Semiconductor facility that processed the DUT and the process if available,

12.2.2 DUT identification number,

12.2.3 Value of *N*,

12.2.4 Value of t_{ox},

12.2.5 Value of G_M,

12.2.6 Irradiation, anneal, and measurement temperatures,

12.2.7 Irradiation biases, and

12.2.8 Whether the drain or source current was used in the calculations.

12.3 For each application of the test method, report the following:

12.3.1 Total dose in rd(SiO_2),

12.3.2 Time between last irradiation and subthreshold measurement,

12.3.3 Anneal bias between last irradiation and subthreshold measurement,

12.3.4 The minimum and maximum subthreshold current values used in the linear least squares fit to find the midgap voltage,

12.3.5 The maximum value of the junction leakage current, and

12.3.6 The values of ΔV_{ot} and ΔV_{it}.

13. Precision and Bias [5]

13.1 *Precision*—An interlaboratory experiment was conducted with five laboratories and the coordinating lab participating. Four additional laboratories had planned on participating but did not complete the study.

13.1.1 Each participating laboratory was asked to perform measurements according to this test method using the samples provided. A sample consisted of a pair of packaged parts, one irradiated to 500 Krad(Si) (plus 24 h 80°C bake) and the second was not irradiated. Each packaged part contained 6 MOSFETs, 3 *n*-channel and 3 *p*-channel MOSFETs (16 µm × 2, 3, and 4 µm). Devices were labeled based on the geometry and type, for example, the unirradiated 2 µm *n*-channel transistor on Sample A is A2*n* and the irradiated 2 µm *n* channel transistor sample is A2*n* (rad). One laboratory tested all nine sample pairs, one laboratory tested four of the nine, and the remaining three laboratories each tested one pair.

13.1.2 The original plan was to assume device-device variations to be insignificant, as all devices came from the same diffusion lot, and to base comparisons on testing done on different samples at the different laboratories. Device-device uniformity, however, was not good, and comparisons were made only where at least three laboratories tested the same device.

13.1.3 Table 2 provides the comparison of Vot and Vit for four devices and four laboratories. The high attrition was due to damaged devices and to devices screened out in accordance with the test method. The worst case standard deviation of the mean measured values was 25 % of the mean, and the 95 % confidence reproducibility limit is 35 %. Although this study did not attempt to measure the repeatability, it is on the order of 1–2 % (dependent on the equipment used to measure I–V characteristics) and is an insignificant component of the precision in this case.

13.1.4 The reproducibility of this test method was determined to be 35 % (95 % confidence limit). The precision is essentially the same as the reproducibility, as the repeatability is insignificant compared to the reproducibility.

13.2 *Bias*—The bias for this test method has not been determined since there is no suitable reference material.

14. Keywords

14.1 c/v characteristics; current–voltage characteristics; interface states; ionizing radiation; MOSFET; oxide-trapped holes; threshold voltage shift; trapped holes

TABLE 2 Interlaboratory Test Data

	Delta Vit (V)				Delta Vot (V)			
Laboratory	A3*n*	A2*n*	F3*n*	A4*p*	A3*n*	A2*n*	F3*n*	A4*p*
1	1.269	1.298	1.282	–0.637	–0.512	–0.479	–0.537	–0.476
2	1.29	1.47	1.29	–1.07	–0.56	–0.59	–0.62	–0.44
3			0.971				–0.546	
4	1.02	1.231		–0.903	–0.603	–0.55		–0.65
Mean	1.193	1.333	1.181	–0.870	–0.558	–0.540	–0.568	–0.522
Standard Deviation	0.150	0.123	0.182	0.218	0.046	0.056	0.046	0.112
Percent sd	12.6 %	9.2 %	15.4 %	25.1 %	8.2 %	10.4 %	8.0 %	21.5 %

[5] Supporting data are available from ASTM Headquarters. Request RR:F01–1014.